ISSN: 0975-766X
CODEN: IJPTFI
Available Online through *Research Article*
www.ijptonline.com

STRUCTURAL EFFECTS OF THE R64W, E167K AND K268R N-ACETYLTRANSFERASE 2 MUTATIONS BY MOLECULAR DYNAMICS SIMULATION

Kavitha.K[1*], Venkataramanan.S[2]
[1]School of Biosciences and Technology (SBST), VIT University, Vellore 632014, Tamil Nadu, India.
[2]Department of Diagnostic and Allied Health Sciences, Management and Science University MSU, Shah Alam 40100, Malaysia.

Received on: 02-02-2017 *Accepted on: 09-03-2017*

Abstract

Human N-acetyltransferase 2 (NAT2) is an important polymorphic catalytic enzyme which metabolizes drugs and chemicals. The polymorphism in NAT2 is often associated with cancer susceptibility and drug toxicity. The functional effect of R64W, E167K and K268R polymorphisms were known, however the structure basis behind these polymorphisms are not clear. Multiple molecular dynamics simulations were performed on these mutations and wildtype to observe the structural and dynamical changes on protein structure, specifically the functionally important regions. The simulation results showed that inter-domain, domain 3 and 17-residue insert regions flexibility reduced relatively to the wild-type. Similarly, the catalytic triad, substrate binding pocket and electrostatic surface of these three mutations completely affected and different from the wild-type. These structural changes on the mutations structure could be responsible for the disruption of their functions. Overall, this study may provide the structural basis for reduced catalytic activity and protein level, as was experimentally observed for these three NAT2 polymorphisms

Keywords: Molecular dynamics simulations, Polymorphism, Drug toxicity, Catalytic triad, Substrate binding pocket.

Introduction

N-acetyltransferases 2 (NAT2, EC 2.3.1.5) is an enzyme play a vital role in phase II xenobiotic metabolism [1-2]. This is a conjugation enzyme mainly catalyzes the transfer of an acetyl group to aromatic amines and hydrazines and this reaction is considered as detoxification process of potentially toxic exogenous compounds[3]. NAT2 is highly polymorphic in nature and characterized in both eukaryotes and prokaryotes [4-5]. The single nucleotide polymorphisms (SNP) which are identified in NAT2 often associated with breast, colon, prostate and urinary bladder cancer [6-12].

Based on allelic variation NAT2 SNPs are classified as rapid, intermediate and slow acetylator phenotypes [13-14]. Understanding the effects of mutations on protein structures often provided vital information about protein dynamics and detailed structural changes which directly reflects to its function [15].

Various computational approaches such as molecular dynamics simulation [16], molecular docking [17-26], protein structure prediction [27-28] and protein modeling are often successful in elucidating the mutational effects on protein structure and dynamics. More specifically molecular dynamics simulation is providing insights about the changes on the structure at picoseconds to milliseconds. Previous study on common seven NAT2 mutations revealed detailed structural changes, specifically the Interdomain (ID) and Domain 3 (D3) flexibility of all seven mutations were reduced compared to the wild-type (WT), changes in the substrate binding pocket and co-factor binding site was observed, and the electropotential surface of all the mutants (MTs) changed drastically compared to WT [15]. Overall these changes in the MTs lead to reduced enzyme activity and reduced protein level.

In this study, we extended the simulation to other three mutations R64W, E167K and K268R. The R64W SNP was reported by Shishikura et al 2000 [29], and Zhu et al investigated the functional study of this mutation [30] that revealed R64W showed reduced protein level, stability and activity. The functional study of E167K in mammalian cells showed reduced protein levels and catalytic activity [13]. The functional study of K286R mutation revealed that the catalytic activity, expression level and protein stability are around 70% compared to other mutations with relative to WT activity [31]. To understand the structural effects of these MTs, Walraven *et al* [32] explored the mutational sites based on crystal structure, however that study did not provide the detailed account on dynamic motion change, substrate binding pocket (SBP) change and orientation change of catalytic site. Therefore, in this study we have used molecular dynamics simulation to elucidate the detailed structural effects caused by these three mutations, we generated MTs structure based on the NAT2 crystal structure and then performed multiple molecular dynamics simulations on MTs and WT. The results showed that the MTs induced structural changes that propagate through space and affect the functionally important regions in the protein structure.

Materials and Methods

Starting structure: The crystal structure of NAT2 (PDB code: 2PFR) was used as starting structure for the WT simulation. The bound coenzyme A and sulphate ion were removed from the crystal structure and then performed 5000

steps (2000 steps of steepest descent and 3000 steps of conjugated gradient) of energy minimization before starting the final simulation. For the MTs structures, respective amino acids were changed on WT structure using Discovery studio 2.5 software and then performed 5000 steps of energy minimization.

Molecular dynamics simulation

Molecular dynamics simulations were performed using the GROMACS software [33] for both WT and MTs. For the simulation and energy minimization GROMOS96 force-field parameters [34] was used. All the structures were solvated in a periodic cubic box with walls extending at least 10 Å from all atoms. In order to neutralize the solvated structures, the GENION program from GROMCAS was used to replace the water molecules with Na^+ and Cl^- ions. The solvated structures were energy minimized with the steepest descent method for 200 ps without using positional restraints and followed by 600 ps of simulation with position restraints. This process was performed mainly to relax the system, then simulation of the full system without any positional restraints for 40,000 ps. Three independent simulations of each protein were performed. All the simulations were performed in the NPT ensemble at a constant temperature (310 K), and the pressure was maintained by coupling to a reference pressure of 1 bar. The non-bonded pair list was updated every 10 steps. The PME algorithm was applied to treat electrostatic interactions. All the bonds were constrained with use of the LINCS algorithm, and the SETTLE algorithm was used to constrain the geometry of the water molecules. A time step of 2 fs was used in all calculations, and coordinates were saved at regular time intervals of every 1 ps.

Analysis of molecular dynamics trajectories

The analysis was performed using last 10 ns structures of each simulation. Structural properties, such as root mean-square deviation (RMSD) and root-mean square fluctuation (RMSF), were calculated with the built-in functions of GROMACS. The analysis of solvent accessible surface area (SASA) was calculated with the NACCESS algorithm [35] and HBPLUS [36] was used for calculating the hydrogen bond interactions. The electrostatic potential was calculated with the Discovery studio 2.5.

Results and Discussions

Mutational effects on NAT2 global structure

MD simulations of R64W, E167K, and K268R MTs were performed at 37ºC and neutral pH in triplicate. The average Cα-RMSD values of each MT from the starting structures were ranging from 1.9 Å to 2.1 Å which was very similar to

the WT simulation indicating that all the MTs are stable throughout the simulation (Table 1). Further, the analysis of total SASA in the MTs showed no increase relative to WT suggesting that the MTs do not expand appreciably during the simulation. It is interesting to observe that the total number of hydrogen bonds in K268R was very close to WT, whereas the other two MTs slightly reduced which may be affect the structural integrity. The last ns structure of each MT indicated that the amino acid substitution does not affect folding or secondary structural elements.

Table 1: General properties of wild-type (WT) and mutant (MT) simulations[a]

Molecule	Cα-RMSD[b] (Å)	Total SASA[c] (Å^2)	Total number of hydrogen bonds
WT[d]	2.0 ± 0.8	13210.17 ± 147.89	264 ± 7
R64W	2.0 ± 0.5	12174.13 ± 136.22	246 ± 6
E167K	1.9 ± 0.3	12716.11 ± 112.91	253 ± 5
K268R	2.1 ± 0.5	12824.19 ± 128.42	258 ± 6

[a]Properties represent averages for 3 simulations over the last 10ns of each simulation.

[b]Cα-RMSD - Root mean square deviation from the starting structure.

[c]SASA - Solvent accessible surface area

[d]Data for WT simulation obtained from our previous study (ref)

Mutational effects on NAT2 structural flexibility

To understand the effects of the mutations on NAT2 structural flexibility, we calculated the RMSF of Cα atoms (Cα-RMSF), which reflects the degree of main-chain fluctuations from the mean structure over the simulation (Figure 3). In the WT simulations, Cα-RMSF values are almost on the same scale and pattern as those of NAT2 crystallographic B-factors. The average Cα-RMSF of WT and MTs simulations was not similar in general (Figure 2). In MTs, specific regions showed either increased or decreased fluctuations relative to the WT. In order to understand the exact percentage of residues having higher flexibility, we calculated the percentage of residues having > 1Å Cα-RMSF value in each domain and this analysis showed D2, ID and D3 from all the MTs showed lesser fluctuation than WT (Table 2).

Table 2: Percentage of residues in each domain with > 1Å Cα-RMSF value calculated in WT and MT simulations.

Molecule	D1[a]	D2[b]	ID[c]	D3[d]
WT[e]	12.8	18.4	28.5	35.0
R64W	21.1	8.6	13.8	20.6
E167K	11.6	14.5	20.2	25.3
K268R	10.4	16.8	26.1	30.6

[a]D1 - Domain 1 (residues 1-83).
[b]D2 - Domain 2 (residues 84-192).
[c]ID - Inter-domain (residues 193-229).
[d]D3 - Domain 3 (residues 230-290).
[e]Data for WT simulation obtained from our previous study (ref)

R64W simulation

Residue R64 is located in the α4-α5 loop in D1, and forms hydrogen bonds with N41, H58 and I59 as well as a salt bridge with E38. Substitution of Trp for Arg breaks the interactions with N41 and E38 (Table 3). These two residues and R64 are highly conserved in NAT proteins, so loss of these interactions may affect the structure and function of this MT severely. The Cα-RMSF analysis showed higher fluctuation around the mutation site, this is mainly due to the loss of hydrogen bond with N41 and salt bridge with E38. Apart from that region, N-terminus, β4-β5 loop in D2 and residues L279-P283 in D3 showed increased fluctuation whereas the remaining region exhibited in lower fluctuation or similar with WT. These fluctuations also have effect on the orientation of the secondary structures such as α3, α4, α5, β2, β5, α9 and α10. Most significant change was observed in α9 and α10 (Figure 3). Formation of a new hydrogen bond by S125/S102 pulled the α9 towards to β2 and β4 and this effect propagated to the α10 where the orientation altered significantly. The orientation change in secondary structures and fluctuations in the different region had large impact on the catalytic triad, SBP and hydrophobic core around SBP. In the catalytic triad, conformation of the residues C68, H106 and D122 was altered which resulted in loss of an important ionic interaction between H106 and D122 (Figure 4). Apart from that, distance between C68 and H106 also increased which may affect the formation of thiolate-imidazolium ion pair. In the SBP, the orientation and the relative position of SBP residues were altered significantly and this leads to complete distortion of the pocket (Figure 5). Further, the analysis of the SBP and hydrophobic core SASA revealed the residues in that region were more buried inside that leads to loss of pocket.

Table 3: Occupancy percentage of the hydrogen bond interactions at the mutation positions in the WT and MTs.

WT[a]	Hb[b]	Occu[c]	MTs	Hb[b]	Occu[c]
R64	9ARG(NH2):::64ARG(O)	18	R64W	64TRP(N):::58HIS(O)	35
	9ARG(NH1):::64ARG(O)	16		64TRP(N):::62ARG(O)	71
	64ARG(NH2):::38GLU(OE2)	87		64TRP(N):::59ILE(O)	15
	64ARG(NH2):::38GLU(OE1)	77		9ARG(NH1):::64TRP(O)	76
	64ARG(NH2):::41ASN(OD1)	88			
	64ARG(N):::58HIS(O)	34			
	64ARG(NH2):::59ILE(O)	51			

E167	249ASN(ND2):::167GLU(OE1)	21	E167K	251ASP(N):::167LYS(O)	92
	251ASN(N):::167GLU(O)	100		167LYS(NZ):::249ASN(OD1)	57
	242ARG(NH2):::167GLU(O)	35		167LYS(NZ):::251ASN(OD2)	42
	167GLU(N):::249ASN(OD1)	64			
	167GLU(N):::249ASN(O)	85			
	185LYS(NZ):::167GLU(OE1)	21			
K268	268LYS(N):::264GLU(O)	100	K268R	268ARG(N):::264GLU(O)	100
	268LYS(N):::265GLU(O)	100		268ARG(N):::264GLU(O)	92
	272LYS(N)::: 268LYS(O)	28			

[a]Data for WT simulation obtained from our previous study (ref)

[b]Hydrogen bonds.

[c]Hydrogen bond occupancy percentage, only occupancies with ≥ 10 in each simulation are shown.

The R64W is a less frequent SNP in Japanese [29] and Korean populations [37]. The functional study of this polymorphism results in reduced enzymatic activity, stability and protein level in the yeast [30]. Loss of important hydrogen bonds and salt bridge are probably affect the stability of the protein [32]. Interestingly, in our study the total number of hydrogen bonds is reduced for this MT, further W64 breaks the interactions with the conserved residues may affect the protein stability. In the previous study, R64Q MT loss of several critical interactions in the mutation site and showed increased flexibility in that region. The R64W mutation also exhibited similar property and also alters the flexibility of the protein in all the domains especially the D2, ID and D3 showed reduced flexibility and also induced local structural change in ID[42]. These changes also affect the packing of catalytic triad residues and SBP residues which results in disruption of the active site. This provides an insight into the structural basis for the decreased activity and stability of this MT.

E167K simulation

Residue E167 is located in β10. In the WT simulation, E167 forms hydrogen bonds with R242, N249, N251 and K185. Substitution of Lys for Glu breaks the interactions with R242 and K185 and loss of these interactions do not increase flexibility around the mutation region. However, this mutation affects the overall flexibility of the protein, except α3-α4 loop, β4-β5 loop and β12-β13 loop the remaining regions showed reduced flexibility than WT (Figure 2). The flexibility changes altered the orientation of the secondary structures such as α3, α4, β4, β4, β12 and the most notable change observed in α9. Formation of the new hydrogen bonds by L209 with F217 and I218 altered the orientation of the helix

(Figure 3). Further, this mutation slightly altered the conformation of the catalytic triad residues (Figure 4). The distance between the H107 and D122 is increased that results in loss of important ionic interaction between them. This mutation also has effect on the SBP. Residues in SBP lost its relative position and orientation that leads to severe distortion of pocket (Figure 5). The SASA analysis in SBP and hydrophobic core around that region further showed that the residues in that region buried more and destroyed the SBP. Although E167 is located in the protein surface it exerts an effect on the protein structure and dynamics. Interestingly, E167 is a starting residue of the 17-residues insert region which is unique for only human NAT2. This insert is away from the catalytic site, so far there is no clear functional role for this insert identified. However, one study suggests that it may contribute to the stability of the protein [38]. In E167K simulation also this insert region showed reduced flexibility compared to the WT indicating that this region might have structural and/or functional importance. The mutation also induces conformational change at the catalytic triad residues and SBP that may affect the activity of the protein. Functional studies of this MT demonstrated a reduced catalytic activity and protein level [13]. Our simulations data explain the possible structural basis for this functional observation.

Table 4: Solvent accessible surface area (SASA) of the substrate binding pocket (SBP) and hydrophobic core around the SBP in WT and MT simulations[a].

Molecule	SASA SBP[b] $(Å)^2$	SASA Hydrophobic Core[c] $(Å)^2$
WT[d]	160.31 ± 22.35	310.76 ± 19.22
R64W	120.11 ± 22.67	225.41 ± 18.33
E167K	126.65 ± 24.22	231.62 ± 19.52
K268R	156.55 ± 22.14	301.17 ± 18.22

[a]SASA were calculated using structures from last 10ns of each simulation.

[b]The following residues were used to calculate the SASA of the SBP site: C68, F93, V106, H107, D122, S125, F217 and S287.

[c]The following residues were used to calculate the SASA of the hydrophobic core around the SBP site: F37, W67, L69, I95, V98, V106, F202, L209, F217 and L288.

[d]Data for WT simulation obtained from our previous study (ref)

K268R simulation

Residue K268 is located in α11 of D3. In the WT simulation, K268 forms hydrogen bonds with E264, E265 and K272, whereas in K268R simulation only with E264 was observed. Substitution of Arg for Lys has little effect on the flexibility

compared to the WT (Figure 2). The Cα-RMSF values of K268R are very close to the WT in many regions. However, the percentage of residues having >1 Å Cα-RMSF values indicated that the ID and D3 has slightly reduced flexibility (Table 2). These slight flexibility changes do not significantly affect the local tertiary structure (Figure 3). The average K268R showed no significant deviation in secondary structures except loops. This mutation has very little effect on the orientation of the catalytic triad residues (Figure 4), however the important ionic interaction between H107 and D122 is observed. Similarly, the SBP do not have any distortion (Figure 5). Further SASA analysis showed that the SBP residues and the hydrophobic core around the SBP are very close to the WT.

This polymorphism is classified as a fast acetylator because of the conservative amino acid substitution [1]. Residue K268 is also located on the surface of the protein and the mutation did not affect the α11 structure. This mutation mostly follows similar pattern as WT in the flexibility and there is no disruption in the packing of tertiary structure, catalytic triad and SBP. Interestingly, the flexibility of the 17-residue inserts regions very close WT. Except this MT remaining all MTs showed reduced flexibility in that region. This again confirms the importance of this insert. Functional study of this MT in different cells [39-40,31,41] showed no reduction in protein expression, stability and catalytic activity. Our simulation data clearly explains why this MT is functionally active.

Figure 1:

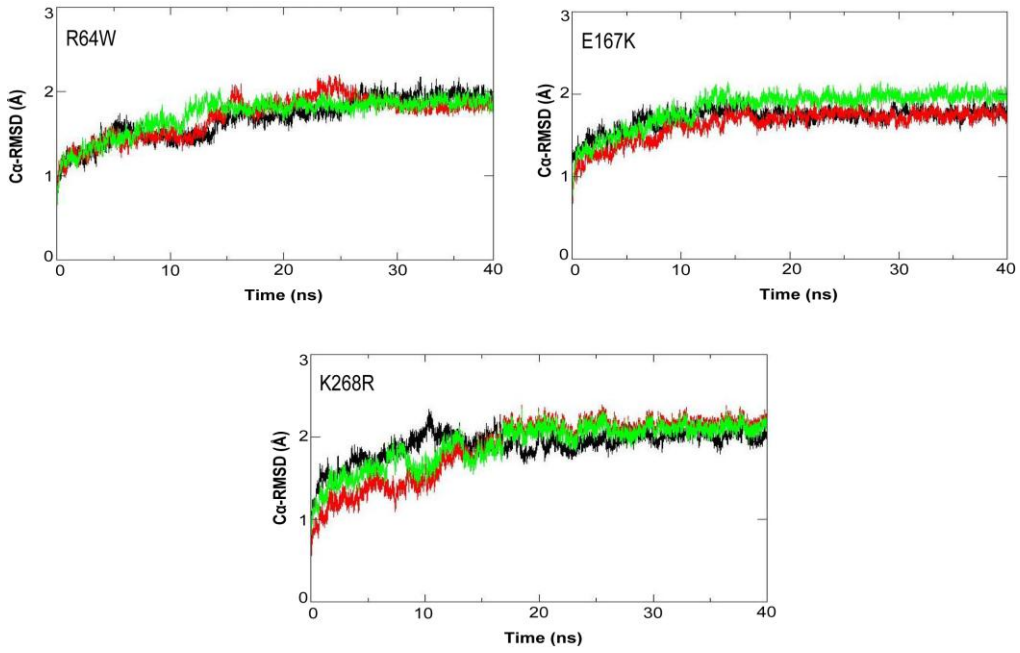

Figure 1- Overall Cα-RMSD of the wild-type (WT) and mutant (MT) structures with respect to the starting structures over 40-ns simulations. Three independent simulations (black, red and green) of each protein were shown.

Figure 2:

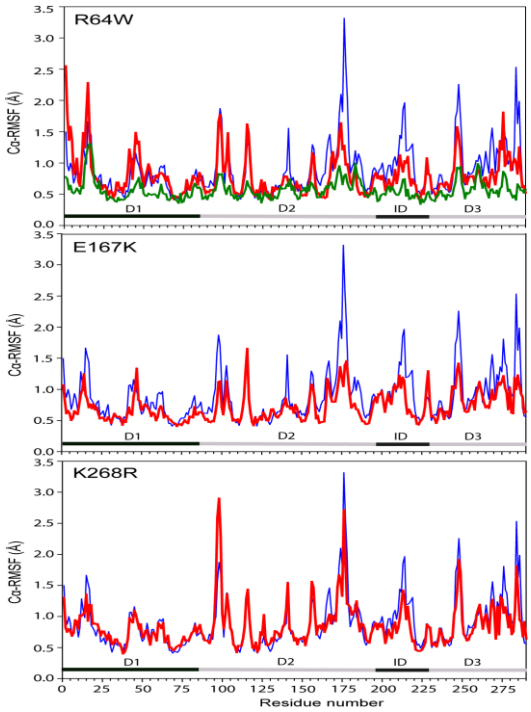

Figure2 - Flexibility of WT and MT structures. Cα-RMSF values (in Å) per residue for the WT (blue) compared with MTs (A) R64W, (B) E167K, and (C) K268R (all in red). Crystallographic *B*-factors from the WT structure (PDB code: 2PFR) are colored in green. The Cα-RMSF values were calculated from the last 10-ns structures of each simulation. Different domains are indicated in alternate black and gray lines at the bottom of the figure.

Figure 3:

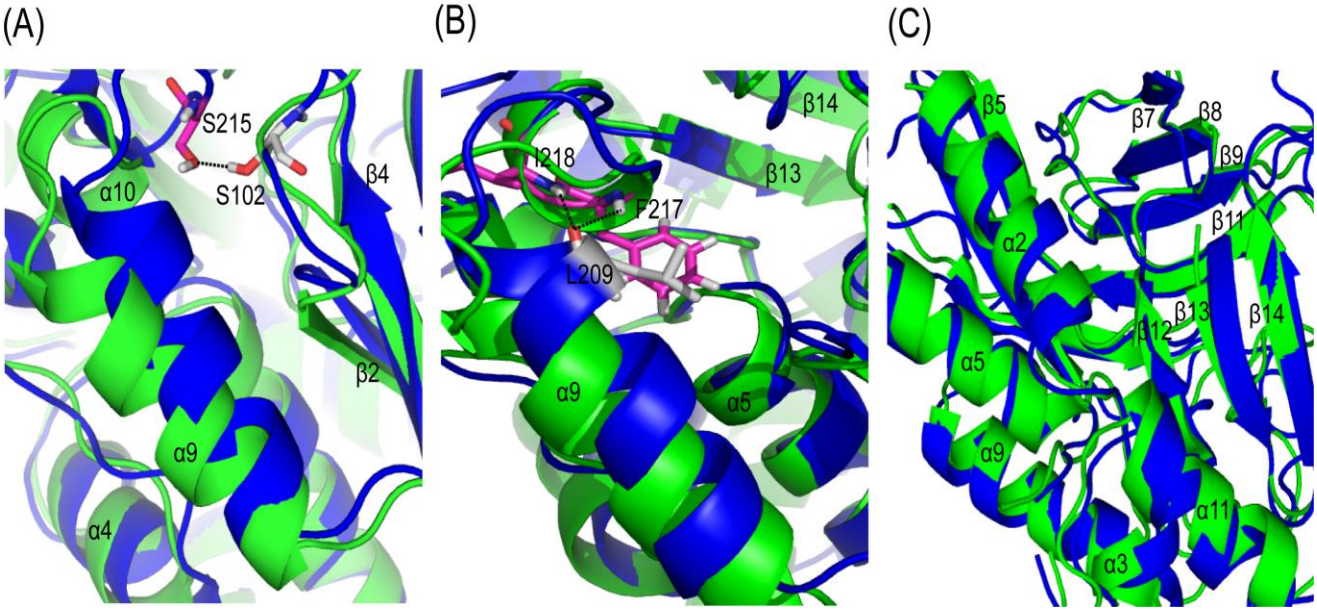

Figure 3 : Tertiary structural changes. The local tertiary structure of the MTs (blue) is superimposed with the WT structure (green). The average structures from last 10-ns of one simulation are shown here. (A) In R64W, new hydrogen bond (S215-S102) is formed, which pull the α9 towards the β2 and β4. (B) In E167K, L209 is formed new hydrogen bonds with F217 and I218 which resulted in alteration of α9 helix orientation. (C) In K286R, there is no significant change in the structure observed.

Figure 4:

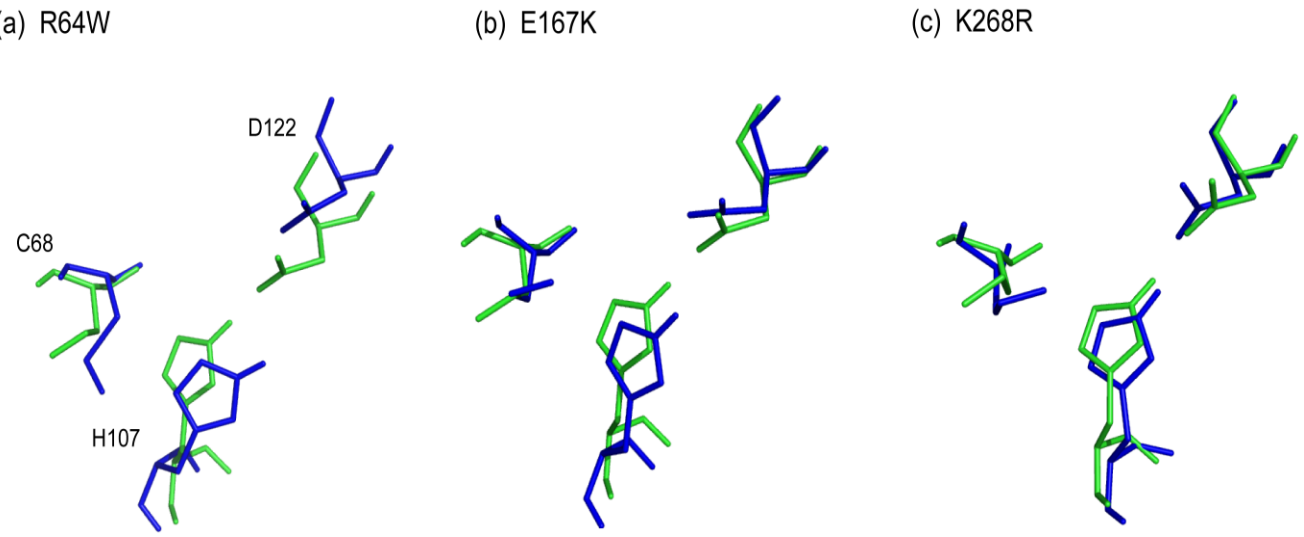

Figure 4- Catalytic triad conformation. (A) R64W, (B) E167K and (C) K286R. The averaged structure from last 10-ns of the simulation of WT (green) is superimposed with each MT (blue) averaged structure.

Figure 5:

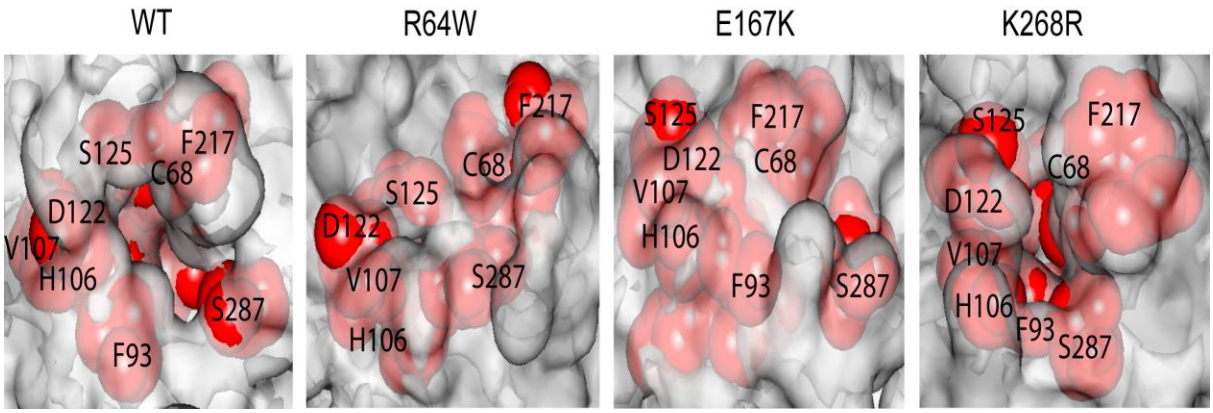

Figure 5- Structural changes on the substrate binding pocket. Molecular surface in the vicinity of the substrate binding pocket of the WT and MTs. The surface portions corresponding to residues involved in forming the substrate binding pocket (C68, F93, V106, H107, D122, S125, F217 and S287) are in red. A cavity is observed only in WT and K268R but not in R64W and E167K. Structures were taken from the snapshot at 40th ns from one simulation

Figure 6:

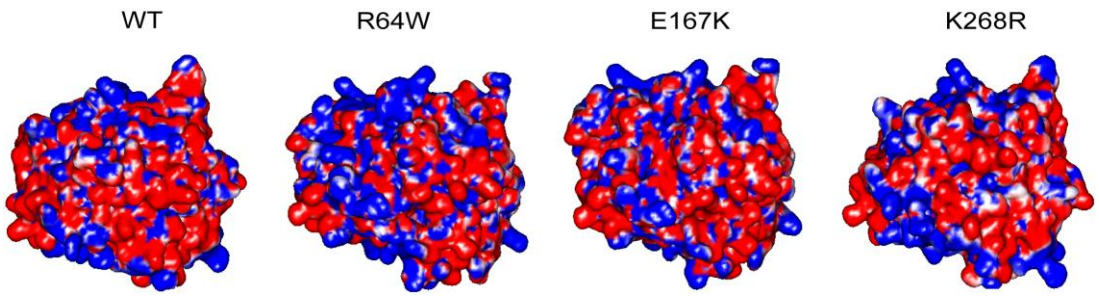

Figure 6 : Electrostatic potential on the surface of WT and MTs. Electronegative and electropositive charges are colored in red and blue, respectively.

Conclusion

We performed MD simulations of the R64W, E167K and K268R NAT2 polymorphisms to study the effects of these mutations on NAT2 structure. Even though R64W and E167K located in different place, they can exert an effect on the protein structure and dynamics especially ID, D3, Catalytic triad and SBP. Interestingly, K268R mutation follows a similar pattern of WT in the flexibility and other structural properties. This gives insight into structural basis for this mutation. In the case of R64W and E167K, follow similar behavior as other MTs which we reported earlier [15]. These mutations alter flexibility of the protein, disrupt the catalytic triad residues conformation and destroy the SBP. Altogether these effects may be responsible for the reduced catalytic activity. These mutations also alter the surface electrostatic properties which may be responsible for the protein degradation.

Acknowledgement

I thank my dear husband as he always helping and friends who helped me always.

Funding Sources

This research did not receive any specific grant from funding agencies in the public, commercial, or not-for-profit sectors.

Declaration

The manuscript is original and is not published or communicated for publication elsewhere in part or full work.

References

1. Boukouvala S, Fakis G (2005) Arylamine N-acetyltransferases: what we learn from genes and genomes. Drug Metab Rev 37 (3):511-564. doi:W3P3435270T21X76 [pii]10.1080/03602530500251204.
2. Rodrigues-Lima F, Dupret JM (2002) In silico sequence analysis of arylamine N-acetyltransferases: evidence for an absence of lateral gene transfer from bacteria to vertebrates and first description of paralogs in bacteria. Biochem Biophys Res Commun 293 (2):783-792. doi:10.1016/S0006-291X(02)00299-1 S0006-291X(02)00299-1 [pii]
3. Riddle B, Jencks WP (1971) Acetyl-coenzyme A: arylamine N-acetyltransferase. Role of the acetyl-enzyme intermediate and the effects of substituents on the rate. J Biol Chem 246 (10):3250-3258
4. Pompeo F, Brooke E, Kawamura A, Mushtaq A, Sim E (2002) The pharmacogenetics of NAT: structural aspects. Pharmacogenomics 3 (1):19-30. doi:PGS030108 [pii] 10.1517/14622416.3.1.19

5. Windmill KF, Gaedigk A, Hall PM, Samaratunga H, Grant DM, McManus ME (2000) Localization of N-acetyltransferases NAT1 and NAT2 in human tissues. Toxicol Sci 54 (1):19-29
6. Risch A, Wallace DM, Bathers S, Sim E (1995) Slow N-acetylation genotype is a susceptibility factor in occupational and smoking related bladder cancer. Hum Mol Genet 4 (2):231-236
7. Le Marchand L, Hankin JH, Wilkens LR, Pierce LM, Franke A, Kolonel LN, Seifried A, Custer LJ, Chang W, Lum-Jones A, Donlon T (2001) Combined effects of well-done red meat, smoking, and rapid N-acetyltransferase 2 and CYP1A2 phenotypes in increasing colorectal cancer risk. Cancer Epidemiol Biomarkers Prev 10 (12):1259-1266
8. Sillanpaa P, Hirvonen A, Kataja V, Eskelinen M, Kosma VM, Uusitupa M, Vainio H, Mitrunen K (2005) NAT2 slow acetylator genotype as an important modifier of breast cancer risk. Int J Cancer 114 (4):579-584. doi:10.1002/ijc.20677
9. van der Hel OL, Peeters PH, Hein DW, Doll MA, Grobbee DE, Kromhout D, Bueno de Mesquita HB (2003) NAT2 slow acetylation and GSTM1 null genotypes may increase postmenopausal breast cancer risk in long-term smoking women. Pharmacogenetics 13 (7):399-407. doi:10.1097/01.fpc.0000054106.48725.87
10. Zhu J, Chang P, Bondy ML, Sahin AA, Singletary SE, Takahashi S, Shirai T, Li D (2003) Detection of 2-amino-1-methyl-6-phenylimidazo[4,5-b]-pyridine-DNA adducts in normal breast tissues and risk of breast cancer. Cancer Epidemiol Biomarkers Prev 12 (9):830-837
11. Costa S, Pinto D, Morais A, Vasconcelos A, Oliveira J, Lopes C, Medeiros R (2005) Acetylation genotype and the genetic susceptibility to prostate cancer in a southern European population. Prostate 64 (3):246-252. doi:10.1002/pros.20241
12. Hein DW, Leff MA, Ishibe N, Sinha R, Frazier HA, Doll MA, Xiao GH, Weinrich MC, Caporaso NE (2002) Association of prostate cancer with rapid N-acetyltransferase 1 (NAT1*10) in combination with slow N-acetyltransferase 2 acetylator genotypes in a pilot case-control study. Environ Mol Mutagen 40 (3):161-167. doi:10.1002/em.10103
13. Zang Y, Doll MA, Zhao S, States JC, Hein DW (2007) Functional characterization of single-nucleotide polymorphisms and haplotypes of human N-acetyltransferase 2. Carcinogenesis 28 (8):1665-1671. doi:bgm085 [pii] 10.1093/carcin/bgm085

14. Grant DM, Hughes NC, Janezic SA, Goodfellow GH, Chen HJ, Gaedigk A, Yu VL, Grewal R (1997) Human acetyltransferase polymorphisms. Mutat Res 376 (1-2):61-70. doi:S0027-5107(97)00026-2 [pii]
15. Rajasekaran M, Abirami S, Chen C (2011) Effects of single nucleotide polymorphisms on human N-acetyltransferase 2 structure and dynamics by molecular dynamics simulation. PLoS One 6 (9):e25801. doi:10.1371/journal.pone.0025801 PONE-D-11-09790 [pii]
16. Rajasekaran M, Chen C (2012) Structural effect of the L16Q, K50E, and R53P mutations on homeodomain of pituitary homeobox protein 2. Int J Biol Macromol 51 (3):305-313. doi:S0141-8130(12)00169-9 [pii] 10.1016/j.ijbiomac.2012.05.008
17. Chou CC, Rajasekaran M, Chen C (2010) An effective approach for generating a three-Cys2His2 zinc-finger-DNA complex model by docking. BMC Bioinformatics 11:334. doi:1471-2105-11-334 [pii]10.1186/1471-2105-11-334
18. Lou YC, Wei SY, Rajasekaran M, Chou CC, Hsu HM, Tai JH, Chen C (2009) NMR structural analysis of DNA recognition by a novel Myb1 DNA-binding domain in the protozoan parasite Trichomonas vaginalis. Nucleic Acids Res 37 (7):2381-2394. doi:gkp097 [pii]10.1093/nar/gkp097
19. Luo SC, Lou YC, Rajasekaran M, Chang YW, Hsiao CD, Chen C (2013) Structural basis of a physical blockage mechanism for the interaction of response regulator PmrA with connector protein PmrD from Klebsiella pneumoniae. J Biol Chem 288 (35):25551-25561. doi:M113.481978 [pii]10.1074/jbc.M113.481978
20. Lou YC, Wang I, Rajasekaran M, Kao YF, Ho MR, Hsu ST, Chou SH, Wu SH, Chen C (2014) Solution structure and tandem DNA recognition of the C-terminal effector domain of PmrA from Klebsiella pneumoniae. Nucleic Acids Res 42 (6):4080-4093. doi:gkt1345 [pii]10.1093/nar/gkt1345
21. Dominguez C, Boelens R, Bonvin AM (2003) HADDOCK: a protein-protein docking approach based on biochemical or biophysical information. J Am Chem Soc 125 (7):1731-1737. doi:10.1021/ja026939x
22. de Vries SJ, van Dijk M, Bonvin AM (2010) The HADDOCK web server for data-driven biomolecular docking. Nat Protoc 5 (5):883-897. doi:nprot.2010.32 [pii] 10.1038/nprot.2010.32
23. Chen R, Li L, Weng Z (2003) ZDOCK: an initial-stage protein-docking algorithm. Proteins 52 (1):80-87. doi:10.1002/prot.10389

24. Ritchie DW (2003) Evaluation of protein docking predictions using Hex 3.1 in CAPRI rounds 1 and 2. Proteins 52 (1):98-106. doi:10.1002/prot.10379
25. Wei SY, Lou YC, Tsai JY, Ho MR, Chou CC, Rajasekaran M, Hsu HM, Tai JH, Hsiao CD, Chen C (2012) Structure of the Trichomonas vaginalis Myb3 DNA-binding domain bound to a promoter sequence reveals a unique C-terminal beta-hairpin conformation. Nucleic Acids Res 40 (1):449-460. doi:gkr707 [pii]10.1093/nar/gkr707
26. Cho AE, Wendel JA, Vaidehi N, Kekenes-Huskey PM, Floriano WB, Maiti PK, Goddard WA, 3rd (2005) The MPSim-Dock hierarchical docking algorithm: application to the eight trypsin inhibitor cocrystals. J Comput Chem 26 (1):48-71. doi:10.1002/jcc.20118
27. Mahalingam R, Peng HP, Yang AS (2014) Prediction of FMN-binding residues with three-dimensional probability distributions of interacting atoms on protein surfaces. J Theor Biol 343:154-161. doi:S0022-5193(13)00519-5 [pii] 10.1016/j.jtbi.2013.10.020
28. Mahalingam R, Peng HP, Yang AS (2014) Prediction of fatty acid-binding residues on protein surfaces with three-dimensional probability distributions of interacting atoms. Biophys Chem 192:10-19. doi:S0301-4622(14)00069-6 [pii]10.1016/j.bpc.2014.05.002
29. Shishikura K, Hohjoh H, Tokunaga K (2000) Novel allele containing a 190C>T nonsynonymous substitution in the N-acetyltransferase (NAT2) gene. Hum Mutat 15 (6):581. doi:10.1002/1098-1004(200006)15:6<581::AID-HUMU17>3.0.CO;2 V
30. Zhu Y, Doll MA, Hein DW (2002) Functional genomics of C190T single nucleotide polymorphism in human N-acetyltransferase 2. Biol Chem 383 (6):983-987. doi:10.1515/BC.2002.105
31. Fretland AJ, Leff MA, Doll MA, Hein DW (2001) Functional characterization of human N-acetyltransferase 2 (NAT2) single nucleotide polymorphisms. Pharmacogenetics 11 (3):207-215
32. Walraven JM, Zang Y, Trent JO, Hein DW (2008) Structure/function evaluations of single nucleotide polymorphisms in human N-acetyltransferase 2. Curr Drug Metab 9 (6):471-486
33. Van Der Spoel D, Lindahl E, Hess B, Groenhof G, Mark AE, Berendsen HJ (2005) GROMACS: fast, flexible, and free. J Comput Chem 26 (16):1701-1718. doi:10.1002/jcc.20291

34. Achary MS, Reddy AB, Chakrabarti S, Panicker SG, Mandal AK, Ahmed N, Balasubramanian D, Hasnain SE, Nagarajaram HA (2006) Disease-causing mutations in proteins: structural analysis of the CYP1B1 mutations causing primary congenital glaucoma in humans. Biophys J 91 (12):4329-4339. doi:S0006-3495(06)72147-6 [pii]10.1529/biophysj.106.085498
35. Hubbard SJ TJ (1993) NACCESS. Department of Biochemistry and Molecular biology, University College of London.,
36. McDonald IK, Thornton JM (1994) Satisfying hydrogen bonding potential in proteins. J Mol Biol 238 (5):777-793. doi:S0022-2836(84)71334-9 [pii] 10.1006/jmbi.1994.1334
37. Fuselli S, Gilman RH, Chanock SJ, Bonatto SL, De Stefano G, Evans CA, Labuda D, Luiselli D, Salzano FM, Soto G, Vallejo G, Sajantila A, Pettener D, Tarazona-Santos E (2007) Analysis of nucleotide diversity of NAT2 coding region reveals homogeneity across Native American populations and high intra-population diversity. Pharmacogenomics J 7 (2):144-152. doi:6500407 [pii] 10.1038/sj.tpj.6500407
38. Walraven JM, Trent JO, Hein DW (2007) Computational and experimental analyses of mammalian arylamine N-acetyltransferase structure and function. Drug Metab Dispos 35 (6):1001-1007. doi:dmd.107.015040 [pii]10.1124/dmd.107.015040
39. Hein DW, Ferguson RJ, Doll MA, Rustan TD, Gray K (1994) Molecular genetics of human polymorphic N-acetyltransferase: enzymatic analysis of 15 recombinant wild-type, mutant, and chimeric NAT2 allozymes. Hum Mol Genet 3 (5):729-734
40. Hein DW, Doll MA, Rustan TD, Ferguson RJ (1995) Metabolic activation of N-hydroxyarylamines and N-hydroxyarylamides by 16 recombinant human NAT2 allozymes: effects of 7 specific NAT2 nucleic acid substitutions. Cancer Res 55 (16):3531-3536
41. Hein DW, Fretland AJ, Doll MA (2006) Effects of single nucleotide polymorphisms in human N-acetyltransferase 2 on metabolic activation (O-acetylation) of heterocyclic amine carcinogens. Int J Cancer 119 (5):1208-1211. doi:10.1002/ijc.21957
42. Elumalai P, Rajasekaran M, Liu HL, Chen C. Investigation of cation-π interactions in sugar-binding proteins. Protoplasma. 2010 Nov;247(1-2):13-24. doi: 10.1007/s00709-010-0132-x. PubMed PMID: 20379838.